

Grand Valley State University
ScholarWorks@GVSU

Peer Reviewed Articles

Chemistry Department

3-30-1999

State to State Ne-CO Rotationally Inelastic Scattering

Stiliana Antonova
Ohio State Univeristy

Ao Lin
Ohio State University

Antonis P. Tsakotellis
Ohio State University

George C. McBane
Grand Valley State University, mcbaneg@gvsu.edu

Follow this and additional works at: https://scholarworks.gvsu.edu/chm_articles

 Part of the [Biological and Chemical Physics Commons](#)

ScholarWorks Citation

Antonova, Stiliana; Lin, Ao; Tsakotellis, Antonis P.; and McBane, George C., "State to State Ne-CO Rotationally Inelastic Scattering" (1999). *Peer Reviewed Articles*. 11.
https://scholarworks.gvsu.edu/chm_articles/11

This Article is brought to you for free and open access by the Chemistry Department at ScholarWorks@GVSU. It has been accepted for inclusion in Peer Reviewed Articles by an authorized administrator of ScholarWorks@GVSU. For more information, please contact scholarworks@gvsu.edu.

State to state Ne–CO rotationally inelastic scattering

Stiliana Antonova,^{a)} Ao Lin, Antonis P. Tsakotellis, and George C. McBane
Department of Chemistry, The Ohio State University, Columbus, Ohio 43210

(Received 1 February 1999; accepted 30 March 1999)

Measurements of state-to-state integral cross sections for rotational excitation of CO by collisions with Ne are reported. The measurements were performed in crossed molecular beams with resonance enhanced multiphoton detection at collision energies of 711 and 797 cm⁻¹. The cross sections display strong interference structure, with a propensity for odd Δj below $\Delta j=10$. Predictions of the *ab initio* potential surface of Moszynski *et al.* [J. Phys. Chem. A **101**, 4690 (1997)] and the new *ab initio* surface of McBane and Cybulski [J. Chem. Phys. **110**, 11734 (1999), preceding paper] are compared to the data. The new surface agrees more closely with the observed interference structure, although significant disagreements remain. © 1999 American Institute of Physics. [S0021-9606(99)01024-7]

I. INTRODUCTION

The quantum mechanical treatment of $T \leftrightarrow R$ energy transfer is now a well established field. The treatment has two main parts: a description of the potential energy surface for the interaction, and an evaluation of the quantum mechanics of nuclear motion on that surface. For atom–rigid rotor collision systems, the latter part can now be handled routinely; at low to moderate collision energies, essentially exact dynamical calculations are practical, while at higher energies a hierarchy of approximations is available whose applicability has been well studied.^{1–3} On the other hand, the construction of accurate potential energy surfaces remains difficult.⁴ Two main approaches are popular. One approach is to adjust parameters in a flexible empirical potential model to fit a set of experimental data. The second is to calculate by electronic structure methods the values of the total energy of the three-atom system at many different nuclear arrangements, and then fit those points with an analytic expression.

The empirical approach suffers two problems. One is the danger that the empirical model might not be sufficiently flexible to describe nature's surface accurately. The other is that the available data are often sensitive to only some regions of the potential surface, so the fit may be poorly constrained in other regions.

The *ab initio* approach suffers from the expense of high-quality electronic structure calculations. For atom–rigid rotor systems, total energies for many tens or even several hundred nuclear arrangements must be evaluated to constrain the surface. Tradeoffs between computational expense and accuracy are required, and the problem becomes rapidly more difficult as the numbers of electrons and nuclei increase.

In an earlier paper, we described scattering experiments on He–CO collisions and comparison with two high-quality potential surfaces.⁵ One surface was purely *ab initio* and the other was an *ab initio*/empirical hybrid. Interference structure in the post-collision rotational distribution proved very

sensitive to details of the potential surface. We have now performed similar experiments with Ne as the collider, and we describe those experiments and corresponding calculations here.

A few experimental studies of the Ne–CO system have appeared. Virial,^{6,7} viscosity,⁸ diffusion,⁹ and thermal diffusion⁹ coefficients are available. They were interpreted with simple isotropic potentials, although the thermal diffusion results did indicate that anisotropic terms in the Ne–CO potential could be important.⁹ Nerf and Sonnenberg reported Ne pressure broadening cross sections in 1975 for the CO $1 \leftarrow 0$ rotational transition at 77, 198, and 294 K.¹⁰ The rotation-vibration infrared spectrum of the weakly bound Ne–CO complex was reported in 1993 by McKellar and co-workers;¹¹ they assigned part of the data by fitting the observed transitions to an empirical energy level expression for a slightly asymmetric rotor. Recently, Walker *et al.* published a pure rotational spectrum¹² and McKellar and Chan reported infrared data on higher excited states.¹³

The first *ab initio* potential energy surface for Ne–CO was published recently by Moszynski *et al.*¹⁴ It was computed using symmetry-adapted perturbation theory (SAPT) with the bond length of CO fixed at its experimental equilibrium value. The SAPT potential surface reproduced the observed infrared spectrum very well. It aided the assignment of a bending combination band and predicted additional transitions. The $\Sigma-\Sigma$ line positions agreed with the experiment within 0.07 cm⁻¹, indicating that the isotropic part of the potential is very accurate in the van der Waals well.

A new *ab initio* potential surface is described and compared to spectroscopic, pressure broadening, and virial coefficient data in the accompanying paper.¹⁵ It was computed by the supermolecule approach with CCSD(T) calculations and fairly large basis sets.

In this paper we present the first study of Ne–CO scattering. We report state-to-state integral scattering cross sections for center of mass collision energies of 711 cm⁻¹ and 797 cm⁻¹. Our measurements probe primarily the anisotropy of the potential's repulsive wall. We compare the results with cross sections computed from the SAPT potential of

^{a)}Present address: Department of Physics, Bryn Mawr College, Bryn Mawr, PA 19010.

Moszynski *et al.*¹⁴ and from the new CCSD(T) potential called S2 by McBane and Cybulski.¹⁵

II. EXPERIMENT

In the experiment, a rotationally cold beam of CO collided with a supersonic Ne beam in a differentially pumped scattering chamber. 2+1 resonance enhanced multiphoton ionization (REMPI) was used to probe the postcollision CO rotational distribution. Detailed descriptions of our crossed molecular beam apparatus and experimental procedure appeared in an earlier paper.⁵

The CO was seeded in argon (5% CO/95% Ar) to help cool its rotational distribution before the collision. In our apparatus, the angle between the CO and Ne beams, and therefore the center of mass collision energy, can be varied by moving one of the molecular beam sources. The experiments reported in this paper were done at intersection angles of 127° and 140°, corresponding to collision energies 711 cm⁻¹ and 797 cm⁻¹, respectively. Finite translational temperatures in the two molecular beams contribute most of the width in the collision energy distribution; we estimate 3 K in the Ar/CO beam and 2 K in the Ne beam, yielding widths σ_E/E of about 4% at the lower energy and about 6% at the higher one.

UV light at 215 nm, typically about 100 $\mu\text{J}/\text{pulse}$, was generated by tripling the visible output of a pulsed dye laser pumped by the second harmonic of an injection seeded, Q-switched Nd:YAG laser. The UV beam entered the scattering chamber in the plane of the molecular beams and was focused in the region of the beam crossing with a 10 cm focal length lens. Its polarization was slightly elliptical, with the long axis nearly perpendicular to the molecular beam plane. A fast photodiode monitored shot-to-shot variations in the pulse energy.

Scattered CO molecules were ionized with 2+1 REMPI through the S branch of the $E^1\Pi \leftarrow X^1\Sigma$ (0,0) band.¹⁶ dc electric fields accelerated the ions through a half-meter flight tube and onto a microsphere plate detector (El-Mul). The amplified output current was mass gated and collected by a Stanford Research Systems gated integrator.

The dye laser and the CO beam valve pulsed at 10 Hz. The Ne valve was opened for two laser shots and left closed for the next two laser shots. At each wavelength we collected eight samples with the Ne beam on and eight with it off.

III. RESULTS

The initial rotational distribution in the CO beam was measured each day; usually between 70% and 75% of the population was in the $j=0$ state and most of the rest was in the $j=1$ state. A small number of molecules remained in the higher rotational levels. This precollision high- j population was smaller than the scattered population for all final levels we report here.

Figure 1 shows the collision-induced changes in CO rotational state densities. The vertical scales are arbitrary. To extract the densities from the recorded spectra we used the expression

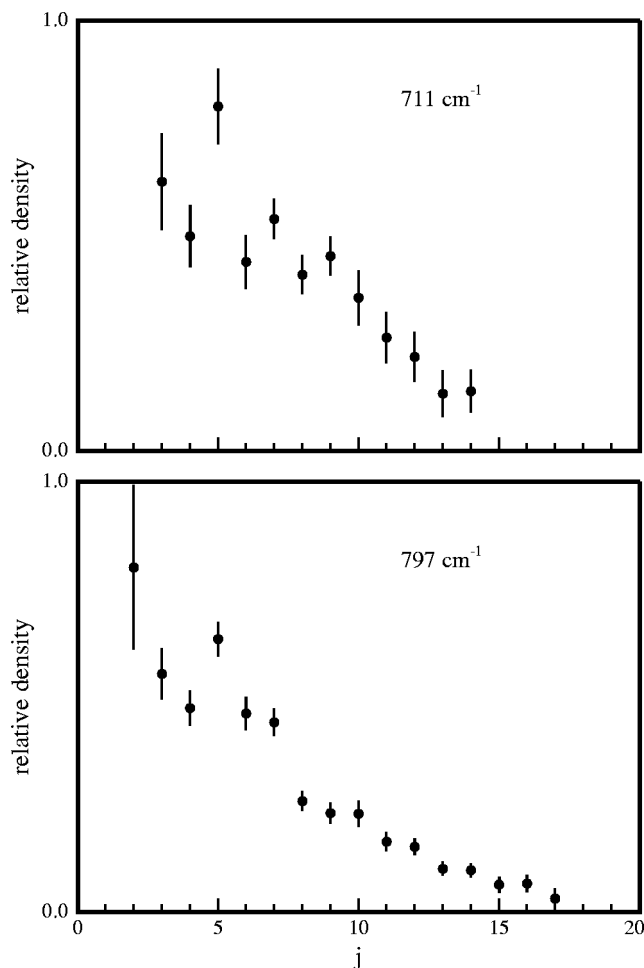


FIG. 1. Relative collision induced densities at the two energies.

$$n(j) \propto \frac{(2j+1)(I_{\text{on}} - I_{\text{off}})}{S_j}, \quad (1)$$

where I_{on} and I_{off} are the areas under the spectral lines with and without the Ne beam. S_j is the rotational line strength factor taken from Bray and Hochstrasser.¹⁷

Each data point in Fig. 1 is a weighted average of several measurements; the error bars indicate two standard deviations in the mean, and represent only random errors. Table I lists the data used in preparing Fig. 1. Data at the two energies have been separately scaled to a maximum density of 0.8.

Etalon effects in the optical path introduced small ($\approx 5\%$), consistent oscillations in the laser pulse energy with wavelength. A comparison between data analyzed with and without corrections for this effect showed that the error introduced into the densities was negligible.

IV. CALCULATIONS

A. Scattering calculations

We calculated integral and differential cross sections for Ne-CO scattering with the MOLSCAT program of Green and Hutson.¹⁸ We used the SAPT potential energy surface of Moszynski *et al.*¹⁴ and the CCSD(T) supermolecule potential S2 of McBane and Cybulski that is described in the accom-

TABLE I. Experimental collision-induced densities and their estimated standard deviations.

j_f	711 cm^{-1}		797 cm^{-1}	
	n_f	S_m	n_f	S_m
2			0.800	
3	0.625	0.055	0.552	0.029
4	0.498	0.035	0.473	0.020
5	0.800		0.634	0.019
6	0.439	0.030	0.461	0.018
7	0.538	0.022	0.440	0.015
8	0.409	0.021	0.257	0.011
9	0.452	0.021	0.229	0.011
10	0.355	0.031	0.228	0.014
11	0.263	0.029	0.163	0.010
12	0.218	0.028	0.151	0.008
13	0.132	0.026	0.100	0.007
14	0.138	0.024	0.096	0.007
15			0.063	0.008
16			0.066	0.009
17			0.031	0.010

panying paper.¹⁵ Moszynski *et al.* describe both a pure *ab initio* surface and a second version with a slightly modified P_2 anisotropic term that fit the infrared data of McKellar *et al.* better. We performed calculations with both surfaces, and found very small differences in their predicted integral cross sections. The results we report here were obtained with the empirically modified surface. All our calculations treated CO as a rigid rotor.

We used the coupled states (CS) approximation of McGuire and Kouri.¹⁹ To check the accuracy of the approximation, we performed a close-coupled (CC) calculation on the SAPT surface at 720 cm^{-1} using total angular momenta from 0 to 99 in steps of 9, and compared the results with a similar CS calculation. Both sets of incomplete cross sections are shown in Fig. 2. The agreement is fairly good. The largest discrepancy appears for $\sigma_{0 \rightarrow 9}$, where the CS approximation overestimates the cross section by about 25%. For most other transitions the CS result is within 10% of the

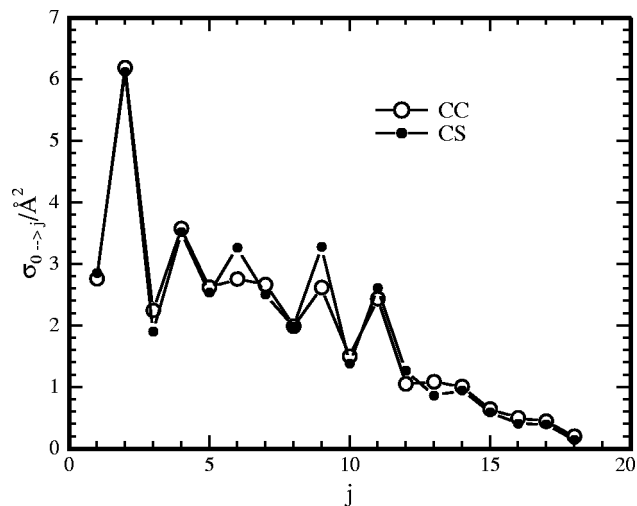


FIG. 2. Incomplete cross sections, accumulated from CC and CS calculations at 720 cm^{-1} with total angular momenta $J=9n$, $n=0\dots 11$.

CC one, and the CS calculations reproduce the correct phase of the even-odd oscillations everywhere. We performed similar test calculations at 290 and 500 cm^{-1} . At the lower energies the CS calculations continued to extract the phase of the even-odd oscillations correctly but many individual cross sections were in error by 20% or more.

All calculations used the hybrid log-derivative/Airy propagator of Alexander and Manolopoulos.²⁰ MOLSCAT's built-in angular expansion routines (the "VRTP mechanism") were used; the potentials were expanded in a basis of Legendre functions $P_l(\cos \theta)$ including terms up through $l=14$, as recommended by Moszynski *et al.* for the SAPT surface. (We found, however, that terms with $l>7$ made only very small contributions to the cross sections.) Twenty-point Gauss-Legendre quadrature was used to evaluate the expansion coefficients. The rotational basis sets included all the open rotational channels and at least two closed channels at each energy. The sum over total angular momentum J terminated at $J=135\hbar$, where the inelastic integral cross sections had converged to better than 0.02 \AA^2 and the elastic cross sections to within 1 \AA^2 at both energies. We performed calculations separately for the two major isotopes of neon (mass numbers 20 and 22) and weighted the results as described below.

B. Density to flux corrections

The REMPI signal measures the number density of molecules in the focal volume of the probe laser, so the experiment is more sensitive to molecules that move slowly in the laboratory. We used the straightforward approach of Dagdigan,²¹ and differential cross sections resulting from the CS calculations, to evaluate the necessary density-to-flux sensitivity factors:

$$\left\langle \frac{g}{v_f} \right\rangle_{if} = \int \left(\frac{g}{v_f} \right) \sigma_{if}^{-1} \left(\frac{d\sigma}{d\omega} \right)_{if} d\omega, \quad (2)$$

where g is the initial relative speed, v_f is the postcollision laboratory speed of a scattered CO molecule, and $\sigma_{if}^{-1}(d\sigma/d\omega)_{if}$ is the normalized differential cross section for the $i \rightarrow f$ transition.

The density to flux corrections are more important in this experiment than our earlier He-CO one, because there is a much wider variation in laboratory speed for different final CO rotational states. The variation in experimental sensitivities $\langle g/v_f \rangle_{if}$ is roughly a factor of 2; the experiment is least sensitive to the lowest rotational levels and most sensitive to $j_f=15$ and 18 at 711 and 797 cm^{-1} , respectively. A more sophisticated evaluation of the sensitivity factors, similar to the approach of Naulin *et al.*²² but extended to arbitrary beam intersection angles and realistic laser focus geometry, gave similar results.

Figure 3 shows the experimental data together with predicted densities calculated from the SAPT and CCSD(T) surfaces. Each predicted density is a weighted sum of four state-to-state integral cross sections, corresponding to the two major isotopes of neon and the two rotational states of CO with significant population in the unscattered beam. The in-

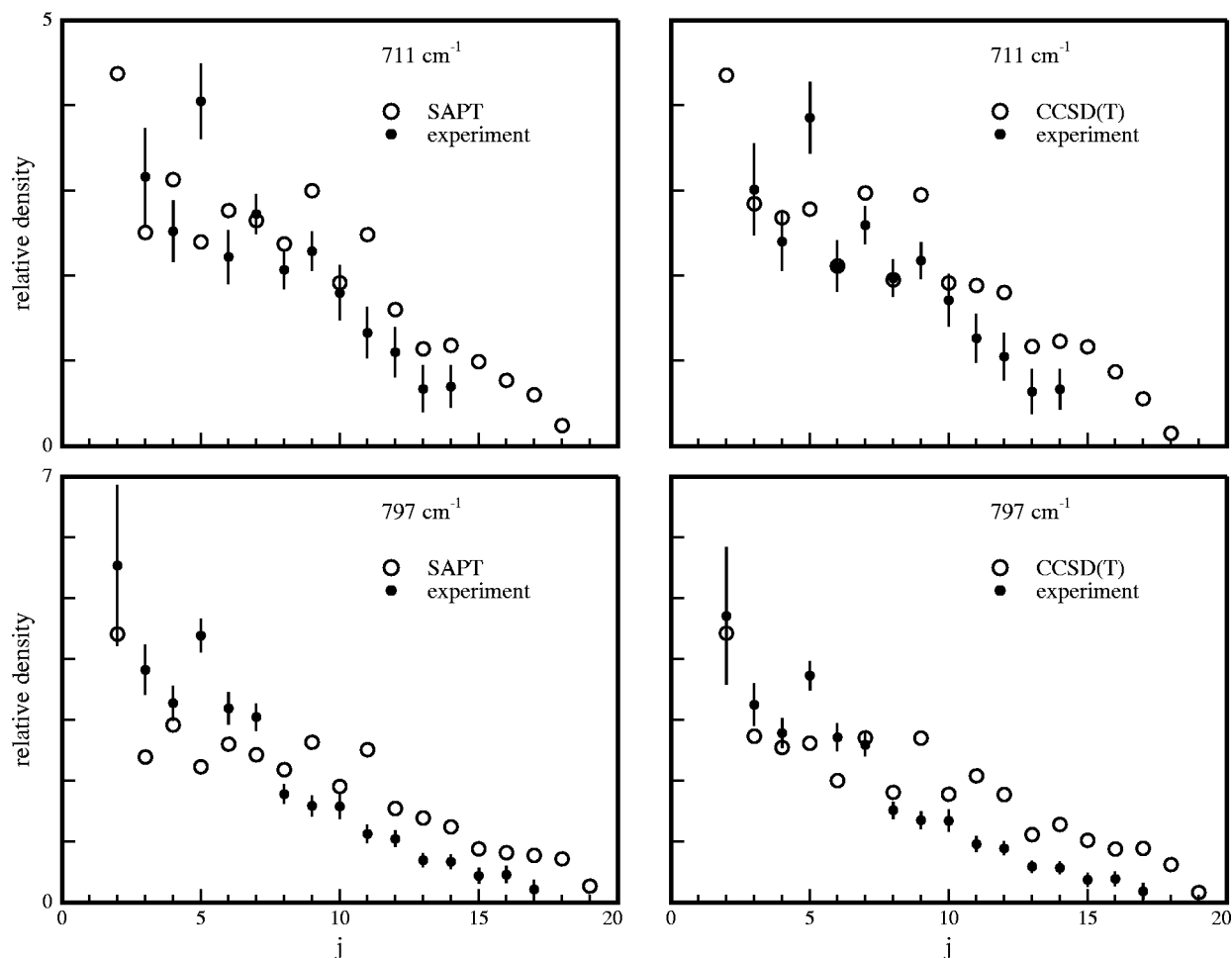


FIG. 3. Experimental results and predictions from the two potential surfaces. The vertical scale is arbitrary, but has been adjusted to correspond approximately to cross sections in \AA^2 for the dominant $0 \rightarrow j$ transitions. The experimental data at each energy were scaled to match the sum of the predicted densities.

tegral cross sections were each multiplied by their own density-to-flux sensitivity factors before weighting. The “theory” points are therefore given by

$$\sigma(j) = f_0 \left(\sigma_{0j}^{20} a_{20} \left\langle \frac{g}{v_f} \right\rangle_{0j}^{20} + \sigma_{0j}^{22} a_{22} \left\langle \frac{g}{v_f} \right\rangle_{0j}^{22} \right) + f_1 \left(\sigma_{1j}^{20} a_{20} \left\langle \frac{g}{v_f} \right\rangle_{1j}^{20} + \sigma_{1j}^{22} a_{22} \left\langle \frac{g}{v_f} \right\rangle_{1j}^{22} \right), \quad (3)$$

with fractional precollision populations $f_0 = 0.75$ and $f_1 = 0.25$ and isotopic abundances $a_{20} = 0.92$ and $a_{22} = 0.08$. The largest contribution comes from the σ_{0j}^{20} integral cross section, which contributes about 70% of the total density.

V. DISCUSSION

A. Comparison of experiment and predictions

The experimental data at 711 cm^{-1} show oscillations in density with j , with clear maxima at $j = 5, 7,$ and 9 , and a roughly monotonic decrease at higher j . At 797 cm^{-1} , the peak at $j = 5$ is prominent, but the peak at $j = 7$ has been reduced to a shoulder and the $j = 9$ density does not stand out at all. The densities decrease in a staircase fashion beyond $j = 8$, suggesting that the propensity may have switched to the even rotational levels at $j = 10, 12,$ and 14 .

The broad decrease in density with j is a nearly universal observation in state-to-state $T \rightarrow R$ transfer; Maricq discussed this trend thoroughly in his 1995 theoretical paper.²³ The even-odd propensity, on the other hand, is an interference effect first identified by Brumer²⁴ and by McCurdy and Miller.²⁵ The interference is related to the rigorous even- Δj requirement in scattering of homonuclear diatomic molecules. In heteronuclear molecules, propensities for either even or odd Δj can appear; the observed propensities are related to the relative importance of terms in the potential with even or odd Legendre orders. Most theoretical studies of this interference effect have used model potential surfaces of the form

$$V(R, \theta) = \sum_{l=0}^2 V_l(R) P_l(\cos \theta) \quad (4)$$

and examined the behavior of predicted propensities as the relative importance of the V_1 and V_2 terms was changed. Experimentally, these interference effects have been observed in collisions of NO ,^{26–29} CN ,^{30–33} and CO .⁵

The densities predicted by the SAPT Ne–CO surface show maxima at $j = 4, 6, 9,$ and 11 for both collision energies. The propensity at low Δj is exactly opposite the experimental one. The CCSD(T) surface does a somewhat better

job of predicting the densities at low Δj ; it gives a shoulder at $j=5$ and maxima at $j=7$ and 9. Neither potential reproduces the strong maximum at $j=5$. The two surfaces agree with each other quite well in the total inelastic cross section and in the rate of falloff with increasing Δj . Above $j=10$ the two potentials show nearly the same behavior; both predict larger densities at rotational levels above $j=11$ than we observe.

B. Origins of disagreement

Discrepancies between theory and experiment could come from errors in the experiment, in the Ne–CO potential surfaces, in the scattering calculations, or in the averaging procedure that relates the calculated cross sections to the measured densities.

1. Systematic experimental errors

We collected ions only at the CO^+ mass, although Hines *et al.* have shown that under some conditions a significant fraction of the ionized CO appears at the C^+ mass.¹⁶ They measured a branching ratio into C^+ of about 5% at low j that varied smoothly with j and decreased with decreasing pulse energy. Their probe pulse energy was about ten times ours; we therefore expect to produce few C^+ ions. In addition, we determined earlier⁵ that no correction for C^+ formation is necessary under our probe conditions.

The most important systematic error in our experiment probably arises from angular momentum alignment in the scattered CO. Several theoretical studies^{34–39} have concluded that diatomic molecules scattered into high j states are likely to have their angular momenta aligned perpendicular to the initial relative velocity. Our detection arrangement is less sensitive to such molecules than to unaligned ones,⁵ so we have probably underestimated the densities at high j . In the limit of perfect negative alignment, we would report a density only 0.6 of the correct value; more likely errors are 10%–20% for $j \approx 15$ and less at lower j . The alignment effect should not vary rapidly with j , as would be required to strongly affect our observed odd- Δj propensity at low Δj . On the other hand, reduced experimental sensitivity from alignment effects probably contributes to the lower ratio of high to low Δj scattering seen in the experiment.

2. Averaging procedure

The procedure for averaging over the initial rotational distribution in the beam and correcting for the density-to-flux transformation, while it is subject to some errors,⁴⁰ does not introduce errors that vary rapidly with j . In the unaveraged $\sigma_{0 \rightarrow j}^{20}$ cross sections, the SAPT potential shows a strong even- Δj propensity while the CCSD(T) potential shows a modest maximum at $\sigma_{0 \rightarrow 5}$ and a strong maximum at $\sigma_{0 \rightarrow 7}$. The average over experimental conditions reduces the amplitude of the oscillations in both potentials, but the qualitative behavior remains the same.

3. Scattering calculations

The scattering calculations are approximate in at least four ways: the numerical solution of the coupled-channel equations, the truncation of the sum over partial waves, the

truncation of the CO rotational basis set, and the use of the coupled states approximation. Convergence tests give us confidence that the first three of these approximations introduce negligible error. The accuracy of the coupled states approximation was discussed above. The comparison with incomplete close-coupled cross sections indicates that CS predicts the phase of the oscillations correctly even though it may introduce small errors in the values of the integral cross sections.

4. Potential surface errors

The most likely source of the discrepancies between theory and experiment at low Δj is errors in the potential surfaces themselves. For the SAPT surface, this conclusion is perhaps not surprising for two reasons. First, the perturbation theory used in construction of the potential surface is more accurate at long range than at short range.⁴ Second, the calculations used by Moszynski *et al.* in constructing their Ne–CO surface extended to a minimum distance of only 5 bohr, while classical trajectories for our collision energies can reach distances as short as 4.7 bohr. A significant part of the dynamics may therefore be occurring on parts of the surface that have been extrapolated from *ab initio* results at larger distances. The CCSD(T) surface was constructed from *ab initio* points that extended farther into the repulsive region, and its absolute accuracy is more or less constant with R ; its errors are probably nearly all due to basis set incompleteness and incomplete treatment of electron correlation. Fitting errors in both surfaces appear to be relatively small.

We performed scattering calculations on several one-parameter modifications of the SAPT surface and found that the even- Δj propensity was remarkably robust toward simpleminded tinkering with the potential. Neither changing the reduced mass of the system nor changing the length scale of the potential by a few percent had any noticeable effect on the even- Δj propensity. Multiplying all the odd- l $V_l(R)$ terms in the potential expansion by some $c \neq 1$ suppressed the even- Δj propensity for $c > 1$ and amplified it for $c < 1$, as we expected from the theoretical work of McCurdy and Miller.²⁵ However, even with $c = 1.2$, the even- Δj propensity remained strong. The modifications have their largest effect at the oxygen end of the molecule. Values of c greater than 1.2 produced unphysical potentials, so we did not pursue this scaling further.

The new CCSD(T) potential comes closer to reproducing the even–odd oscillations at low Δj , but it still does not predict the strong maximum at $\Delta j=5$; in the unaveraged $\sigma_{0 \rightarrow j}^{20}$ cross sections, $\sigma_{0 \rightarrow 7}^{20}$ is a local maximum. This comparison suggests that while its repulsive wall is more accurate than the SAPT one, neither of the two surfaces is as accurate as the best He–CO surfaces.^{41,42}

Since we are attempting to judge the accuracy of the two surfaces by measuring the phase of the interference in the rotational excitation cross sections, it is important to determine whether both surfaces are on the same “interference fringe.” That is, if the propensity changes from even to odd Δj many times as a model surface changes continuously from the SAPT to the CCSD(T) surface, then the improved

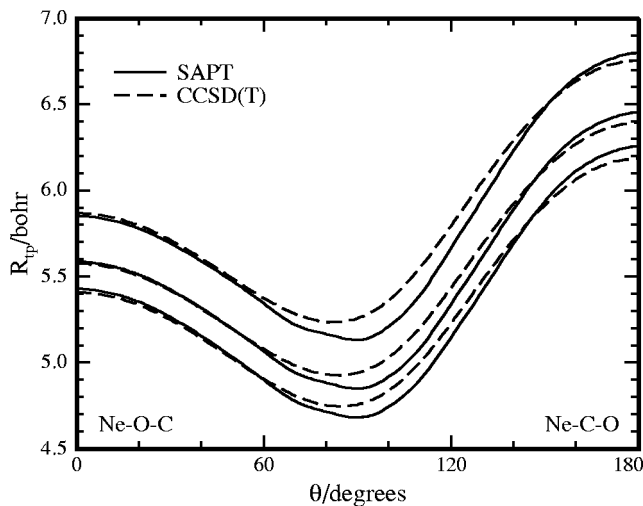


FIG. 4. Potential energy contours for the two Ne-CO potentials at 200, 500, and 800 cm^{-1} . 0° in the figure corresponds to the Ne-O-C arrangement.

agreement of the latter with our observations might be accidental. We carried out scattering calculations on four model surfaces obtained by taking different linear combinations of the SAPT and CCSD(T) energies at each nuclear arrangement. The results showed a smooth, monotonic change from even toward odd Δj propensity as the model surface varied from the SAPT shape to the CCSD(T) shape. On this basis we claim that the improved agreement of the CCSD(T) does represent a real improvement in the shape of the repulsive wall.

C. Comparison of surfaces

Figure 4 displays the 200, 500, and 800 cm^{-1} contours of both the Ne-CO potentials. They are qualitatively similar. There is a "knee" [position of large second derivative in $R_{ep}(\theta)$] in the SAPT potential that does not appear in the other. The SAPT potential allows closer approach in the T arrangement and the CCSD(T) potential allows closer approach at the carbon end of CO. The turning points in the Ne-O-C arrangement are very similar in the two potentials, so the two ends of the CO molecule are more similar in the CCSD(T) potential.

It is interesting that none of the differences between these two potentials should obviously produce a dramatic change from even to odd Δj . In our earlier He-CO work,⁵ we speculated that the difference between the distances of closest approach at the two ends of CO might serve as an indicator of the overall "oddness" of the potential and be reflected in the even-odd propensity. That speculation was clearly too simplistic; exactly the opposite case appears here. The even-odd propensity is controlled by fairly subtle features of the potentials in the repulsive region.

VI. SUMMARY

We have measured state-to-state, rotationally inelastic, relative cross sections for Ne-CO scattering at two collision energies. Cross sections calculated from two different *ab initio* potential surfaces were compared with the data. Both surfaces predicted more scattering into high rotational levels

than was observed; this difference is probably due at least in part to angular momentum alignment, which was not allowed for in the analysis. In addition, the SAPT potential surface predicts an incorrect phase for the interference oscillations in the low Δj cross sections, while the new CCSD(T) surface agrees qualitatively with the experiment at low Δj . This difference is probably due to residual errors in the SAPT surface in the repulsive region.

ACKNOWLEDGMENTS

The authors are grateful to S. M. Cybulski, A. van der Avoird, and R. Moszynski for computer programs evaluating their potential surfaces and for many useful discussions, and to J. M. Hutson and the late S. Green for their MOLSCAT program. Acknowledgement is made to the Donors of The Petroleum Research Fund, administered by the American Chemical Society, for support of this research. Additional support from the Department of Chemistry at Ohio State University and the Ohio Supercomputer Center is gratefully acknowledged.

- ¹J. N. Murrell and S. D. Bosanac, *Introduction to the Theory of Atomic and Molecular Collisions* (Wiley, Chichester, England, 1989).
- ²D. J. Kouri, in *Atom-Molecule Collision Theory: A Guide for the Experimentalist*, edited by R. B. Bernstein (Plenum, New York, 1979), Chap. 9.
- ³D. Secrest, in *Atom-Molecule Collision Theory: A Guide for the Experimentalist*, edited by R. B. Bernstein (Plenum, New York, 1979), Chap. 8.
- ⁴A. J. Stone, *The Theory of Intermolecular Forces, The International Series of Monographs in Chemistry* (Clarendon, Oxford, 1996).
- ⁵S. Antonova, A. Lin, A. P. Tsakotellis, and G. C. McBane, *J. Chem. Phys.* **110**, 2384 (1999).
- ⁶J. Brewer, AFOSR Technical Report MRL-2915-C, 1967; R. Moszynski, T. Korona, T. G. A. Heijmen, P. E. S. Wormer, A. van der Avoird, and B. Schramm, *Pol. J. Chem.* **72**, 1479 (1998).
- ⁷K. Vatter, H. J. Schmidt, E. Elias, and B. Schramm, *Ber. Bunsenges. Phys. Chem.* **100**, 73 (1996).
- ⁸J. Kestin, S. T. Ro, and W. A. Wakeham, *Ber. Bunsenges. Phys. Chem.* **86**, 753 (1982).
- ⁹R. D. Trengrove, H. L. Robjohns, and P. J. Dunlop, *Ber. Bunsenges. Phys. Chem.* **88**, 450 (1984).
- ¹⁰R. B. Nerf, J. and M. A. Sonnenberg, *J. Mol. Spectrosc.* **58**, 474 (1975).
- ¹¹R. W. Randall, A. J. Cliffe, B. J. Howard, and A. R. W. McKellar, *Mol. Phys.* **79**, 1113 (1993).
- ¹²K. A. Walker, T. Ogata, W. Jäger, M. C. L. Gerry, and I. Ozier, *J. Chem. Phys.* **106**, 7519 (1997).
- ¹³A. R. W. McKellar and M. C. Chan, *Mol. Phys.* **93**, 253 (1998).
- ¹⁴R. Moszynski, T. Korona, P. E. S. Wormer, and A. van der Avoird, *J. Phys. Chem. A* **101**, 4690 (1997).
- ¹⁵G. C. McBane and S. M. Cybulski, *J. Chem. Phys.* **110**, 11734 (1999), preceding paper.
- ¹⁶M. A. Hines, H. A. Michelsen, and R. N. Zare, *J. Chem. Phys.* **93**, 8557 (1990).
- ¹⁷R. G. Bray and R. M. Hochstrasser, *Mol. Phys.* **31**, 1199 (1976).
- ¹⁸J. M. Hutson and S. Green, MOLSCAT computer code, version 14 (1994), distributed by Collaborative Computational Project No. 6 of the Engineering and Physical Sciences Research Council (U.K.).
- ¹⁹P. McGuire and D. J. Kouri, *J. Chem. Phys.* **60**, 2488 (1974).
- ²⁰M. H. Alexander and D. E. Manolopoulos, *J. Chem. Phys.* **86**, 2044 (1987).
- ²¹P. J. Dagdigian, in *Atomic and Molecular Beam Methods, Vol. I*, edited by G. Scoles (Oxford University Press, New York, 1988).
- ²²C. Naulin, M. Costes, A. Benseddik, and G. Dorthe, *Laser Chem.* **8**, 283 (1988).
- ²³M. M. Maricq, *J. Chem. Phys.* **103**, 5999 (1995).
- ²⁴P. Brumer, *Chem. Phys. Lett.* **28**, 345 (1974).
- ²⁵C. W. McCurdy and W. H. Miller, *J. Chem. Phys.* **67**, 463 (1977).
- ²⁶P. Andresen, H. Joswig, H. Pauly, and R. Schinke, *J. Chem. Phys.* **77**, 2204 (1982).
- ²⁷H. Joswig, P. Andresen, and R. Schinke, *J. Chem. Phys.* **85**, 1904 (1986).
- ²⁸A. V. Smith and A. W. Johnson, *Chem. Phys. Lett.* **93**, 608 (1982).

- ²⁹H. Meyer, *J. Phys. Chem.* **99**, 1101 (1995).
- ³⁰R. Fei, H. M. Lambert, T. Carrington, S. V. Filseth, C. M. Sadowski, and C. H. Dugan, *J. Chem. Phys.* **100**, 1190 (1994).
- ³¹N. Furio, A. Ali, and P. J. Dagdigian, *J. Chem. Phys.* **85**, 3860 (1986).
- ³²G. Jihua, A. Ali, and P. J. Dagdigian, *J. Chem. Phys.* **85**, 7098 (1986).
- ³³P. J. Dagdigian, D. Patel-Misra, A. Berning, H.-J. Werner, and M. H. Alexander, *J. Chem. Phys.* **98**, 8580 (1993).
- ³⁴M. H. Alexander and P. J. Dagdigian, *J. Chem. Phys.* **66**, 4126 (1977).
- ³⁵M. H. Alexander, *J. Chem. Phys.* **67**, 2703 (1977).
- ³⁶T. Orlikowski and M. H. Alexander, *J. Chem. Phys.* **80**, 4133 (1984).
- ³⁷H. R. Mayne and M. Keil, *J. Phys. Chem.* **88**, 883 (1984).
- ³⁸B. Follmeg, P. Rosmus, and H.-J. Werner, *J. Chem. Phys.* **93**, 4687 (1990).
- ³⁹D. Pullman, B. Friedrich, and D. Herschbach, *J. Phys. Chem.* **99**, 7407 (1995).
- ⁴⁰D. M. Sonnenfroh and K. Liu, *Chem. Phys. Lett.* **176**, 183 (1991).
- ⁴¹R. J. Le Roy, C. Bissonnette, T. H. Wu, A. K. Dham, and W. J. Meath, *Faraday Discuss.* **97**, 81 (1994).
- ⁴²T. G. A. Heijmen, R. Moszynski, P. E. S. Wormer, and A. van der Avoird, *J. Chem. Phys.* **107**, 9921 (1997).